

## X-RAY, UV, AND OPTICAL OBSERVATIONS OF SUPERNOVA 2006bp WITH SWIFT: DETECTION OF EARLY X-RAY EMISSION

S. IMMLER<sup>1,2</sup>, P. J. BROWN<sup>3</sup>, P. MILNE<sup>4</sup>, L. DESSART<sup>4</sup>, P. A. MAZZALI<sup>5,6</sup>, W. LANDSMAN<sup>1</sup>, N. GEHRELS<sup>7</sup>, R. PETRE<sup>1</sup>, D. N. BURROWS<sup>3</sup>, J. A. NOUSEK<sup>3</sup>, R. A. CHEVALIER<sup>8</sup>, C. L. WILLIAMS<sup>1</sup>, M. KOSS<sup>1</sup>, C. J. STOCKDALE<sup>9</sup>, M. T. KELLEY<sup>9</sup>, K. W. WEILER<sup>10</sup>, S. T. HOLLAND<sup>1,2</sup>, E. PIAN<sup>5</sup>, P. W. A. ROMING<sup>3</sup>, D. POOLEY<sup>11,12</sup>, K. NOMOTO<sup>13</sup>, J. GREINER<sup>14</sup>, S. CAMPANA<sup>15</sup>, AND A. M. SODERBERG<sup>16</sup>

*Draft version May 26, 2022*

### ABSTRACT

We present results on the X-ray and optical/UV emission from the type IIP supernova (SN) 2006bp and the interaction of the SN shock with its environment, obtained with the X-Ray Telescope (XRT) and UV/Optical Telescope (UVOT) on-board the *Swift* observatory. SN 2006bp is detected in X-rays at a  $4.5\sigma$  level of significance in the merged XRT data from days 1 to 12 after the explosion. If the (0.2–10 keV band) X-ray luminosity of  $L_{0.2-10} = (1.8 \pm 0.4) \times 10^{39}$  ergs s<sup>-1</sup> is caused by interaction of the SN shock with circumstellar material (CSM), deposited by a stellar wind from the progenitor's companion star, a mass-loss rate of  $\dot{M} \approx 1 \times 10^{-5} M_{\odot} \text{ yr}^{-1}$  ( $v_w/10 \text{ km s}^{-1}$ ) is inferred. The mass-loss rate is consistent with the non-detection in the radio with the *VLA* on days 2, 9, and 11 after the explosion and characteristic of a red supergiant progenitor with a mass around  $\approx 12\text{--}15 M_{\odot}$  prior to the explosion. The *Swift* data further show a fading of the X-ray emission starting around day 12 after the explosion. In combination with a follow-up *XMM-Newton* observation obtained on day 21 after the explosion, an X-ray rate of decline  $L_x \propto t^{-n}$  with index  $n = 1.2 \pm 0.6$  is inferred. Since no other SN has been detected in X-rays prior to the optical peak and since type IIP SNe have an extended 'plateau' phase in the optical, we discuss the scenario that the X-rays might be due to inverse Compton scattering of photospheric optical photons off relativistic electrons produced in circumstellar shocks. However, due to the high required value of the Lorentz factor ( $\approx 10\text{--}100$ ), inconsistent with the ejecta velocity inferred from optical line widths, we conclude that Inverse Compton scattering is an unlikely explanation for the observed X-ray emission. The fast evolution of the optical/ultraviolet (1900–5500Å) spectral energy distribution and the spectral changes observed with *Swift* reveal the onset of metal line-blanketing and cooling of the expanding photosphere during the first few weeks after the outburst.

*Subject headings:* stars: supernovae: individual (SN 2006bp) — stars: circumstellar matter — X-rays: general — X-rays: individual (SN 2006bp) — X-rays: ISM — ultraviolet: ISM

### 1. INTRODUCTION

SN 2006bp was discovered on April 9.6, 2006, with an apparent magnitude of 16.7 in unfiltered 20-s CCD exposures using a 0.60-m *f*/5.7 reflector (Nakano & Itagaki 2006). Subsequent observations by Itagaki showed that the SN brightened rapidly between April 9.6 and 9.8 UT. The non-detection in unfiltered ROTSE-IIIb observations on April 9.15 UT ( $> 16.9$  mag; Quimby et al. 2006) give a likely explosion date of April 9, 2006. Based on the optical/UV colors (Immler, Brown & Milne 2006) observed with *Swift* and the detection of hydrogen and helium lines in ground-based optical spectra (Quimby et al. 2006), SN 2006bp was classified as a core-collapse type II SN.

The optical/UV lightcurve established by *Swift* (this work) shows that SN 2006bp belongs to the class of type IIP SNe which are characterized by a prolonged 'plateau' period of sustained optical flux (see Sec. 3.1). This plateau phase results from recombination in the massive hydrogen envelopes ( $\gtrsim 2M_{\odot}$  H mass) of the progenitors. Most massive stars ( $\approx 8\text{--}25 M_{\odot}$ ) become

I-23807 Merate, Italy

<sup>16</sup> Division of Physics, Mathematics, and Astronomy, California Institute of Technology, MS 105-24, Pasadena, CA 91125

Electronic address: stefan.m.immler@nasa.gov

<sup>1</sup> Astrophysics Science Division, X-Ray Astrophysical Laboratory, Code 662, NASA Goddard Space Flight Center, Greenbelt, MD 20771

<sup>2</sup> Universities Space Research Association, 10211 Wincopin Circle, Columbia, MD 21044

<sup>3</sup> Department of Astronomy and Astrophysics, Pennsylvania State University, 525 Davey Laboratory, University Park, PA 16802

<sup>4</sup> Steward Observatory, 933 North Cherry Avenue, RM N204 Tucson, AZ 85721

<sup>5</sup> INAF, Osservatorio Astronomico di Trieste, via G.B. Tiepolo 11, 34131 Trieste, Italy

<sup>6</sup> Max-Planck-Institut für Astrophysik, Karl-Schwarzschild Strasse 1, 85741 Garching, Germany

<sup>7</sup> Astrophysics Science Division, Astroparticle Physics Laboratory, Code 661, NASA Goddard Space Flight Center, Greenbelt, MD 20771

<sup>8</sup> Department of Astronomy, University of Virginia, P.O. Box 400325, Charlottesville, VA 22904

<sup>9</sup> Department of Physics, Marquette University, P.O. Box 1881, Milwaukee, WI 53201-1881

<sup>10</sup> Naval Research Laboratory, Code 7210, Washington, DC 20375-5320

<sup>11</sup> Astronomy Department, University of California at Berkeley, 601 Campbell Hall, Berkeley, CA 9472

<sup>12</sup> Chandra Fellow

<sup>13</sup> Department of Astronomy, School of Science, University of Tokyo, Bunkyo-ku, Tokyo 113-0033, Japan

<sup>14</sup> Max-Planck-Institut für extraterrestrische Physik, Giessenbachstrasse, 85748 Garching, Germany

<sup>15</sup> INAF - Osservatorio Astronomico di Brera, via E. Bianchi 46,

type II SNe, approximately 2/3 of which are type IIP (Heger et al. 2003) depending on the mass and metallicity. Due to the large masses of the progenitor stars and high abundance of type IIP SNe, they play a primary role in the formation of neutron stars. Such massive progenitor stars have strong stellar winds which can deposit significant amounts of material in their environments. As the outgoing SN shock runs through the CSM deposited by the stellar wind, large amounts of X-ray emission and radio synchrotron emission can be produced. Four of the 26 SNe detected in X-rays to date<sup>17</sup> are type IIP: SNe 1999em, 1999gi, 2002hh, and 2004dj (see Tables 1, 2 and references in Chevalier et al. 2006). Mass-loss rate estimates from the X-ray and radio observations are between a few  $\times 10^{-6}$  to  $10^{-5} M_{\odot} \text{ yr}^{-1}$  ( $v_w/10 \text{ km s}^{-1}$ ), where  $v_w$  is the pre-SN stellar wind velocity.

In this paper we present the earliest observation and detection of a SN in X-rays to date, starting one day after the explosion. In addition to the *Swift* X-ray and a follow-up *XMM-Newton* X-ray observation, we discuss the broad-band spectral energy distribution during the early evolution (days to weeks) of SN 2006bp, as well as multi-epoch UV spectra obtained with *Swift*.

## 2. OBSERVATIONS

### 2.1. *Swift* UVOT Optical/UV Observations

The Ultraviolet/Optical Telescope (UVOT; Roming et al. 2005) and X-Ray Telescope (XRT, Burrows et al. 2005) on-board the *Swift* Observatory (Gehrels et al. 2004) began observing SN 2006bp on April 10.54 UT. The HEASOFT<sup>18</sup> (version 6.1.1) and *Swift* Software (version 2.5, build 19) tools and latest calibration products were used to analyze the data.

The SN was detected with the UVOT at R.A. = 11h53m55s.70, Decl. = +52°21'10".4 (equinox 2000.0), with peak magnitudes of  $V = 15.1$ ,  $B = 15.4$ ,  $U = 14.5$ ,  $UVW1$  [216–286 nm FWHM] = 14.7,  $UVM2$  [192–242 nm] = 15.1, and  $UVW2$  [170–226 nm] = 14.8. Statistical and systematic errors are 0.1 mag each.

Based on the UVOT photometry and  $V - B$  and  $B - U$  colors, the SN was classified as a young type II event (Immler, Brown & Milne 2006). The classification was confirmed by Hobby-Eberly Telescope (HET) spectra taken on day 2, showing a blue continuum and a narrow absorption line at 592 nm, consistent with Na I in the host galaxy NGC 3953 rest frame ( $z = 0.00351$ , Verheijen & Sancisi 2001), a narrow emission line consistent with rest-frame H $\alpha$ , a broad absorption line around 627 nm, and a narrow but slightly broadened emission line at 583 nm (Quimby et al. 2006).

Thirty-five individual exposures were obtained between April 10.54 UT and May 30.45 UT (see Table 1 for an observation log). Assuming an explosion date of April 9, the observations correspond to days 1–51 after the explosion.

*Swift* optical, UV, and X-ray images of SN 2006bp and its host galaxy NGC 3953 (Hubble type SBbc; NED) are shown in Fig. 1. The UVOT 6-filter lightcurve of SN 2006bp is given in Fig. 2.

TABLE 1  
*Swift* OBSERVATIONS OF 2006BP

Sequence	Date	XRT Exp	UVOT Exp
(1)	[UT]	[s]	[s]
30390001	2006-04-10 12:47:26	4333	4917
30390003	2006-04-11 03:22:00	4323	4301
30390004	2006-04-12 08:19:01	3157	2770
30390005	2006-04-12 03:30:00	1705	1684
30390006	2006-04-13 03:37:00	6906	6660
30390007	2006-04-14 08:38:01	748	746
30390008	2006-04-14 16:39:01	868	899
30390009	2006-04-14 08:34:01	156	155
30390010	2006-04-14 16:36:01	4	4
30390011	2006-04-15 07:06:01	3373	3296
30390012	2006-04-15 18:22:01	1572	1544
30390013	2006-04-16 05:36:00	260	260
30390014	2006-04-16 18:29:00	80	81
30390015	2006-04-16 05:39:01	3013	2995
30390016	2006-04-16 18:30:02	1537	1526
30390017	2006-04-17 04:04:01	3666	3494
30390018	2006-04-17 18:35:01	1639	1612
30390019	2006-04-18 07:23:00	61	57
30390020	2006-04-18 07:27:01	2609	2935
30390021	2006-04-20 14:00:01	3174	3118
30390022	2006-04-21 06:04:01	363	364
30390023	2006-04-21 06:09:01	2741	2743
30390024	2006-04-22 02:57:00	2801	2749
30390025	2006-04-23 03:03:01	742	743
30390026	2006-04-23 03:07:01	5248	5221
30390027	2006-04-24 01:32:01	2999	2733
30390028	2006-04-26 01:43:00	1782	1642
30390029	2006-04-28 00:50:01	2829	2693
30390030	2006-05-01 10:14:01	974	965
30390031	2006-05-01 11:50:01	3793	3914
30390032	2006-05-04 04:06:01	2542	2450
30390034	2006-05-10 00:21:40	884	873
30390036	2006-05-22 12:17:00	622	863
30390037	2006-05-22 12:34:01	633	976
30390038	2006-05-30 08:32:01	5242	5143

NOTE. — (1) *Swift* sequence number; (2) Date in units of Universal Time (UT); (3) X-Ray Telescope (XRT) exposure time in units of s; (4) Ultraviolet/Optical Telescope (UVOT) exposure time in units of s.

### 2.2. *Swift* Grism Observations

The UVOT includes two grisms for obtaining spectra in the UV and visible bands. The UV grism has a nominal wavelength range of 1800–2900 Å, while the V grism has a wavelength range of 2800–5200 Å. The UV grism also records spectra in the 2900–4900 Å range, but at half the sensitivity of the V grism, and with the possibility of contamination by second order overlap. We obtained six UV grism spectra and one V grism spectrum of SN 2006bp. The four earlier grism observations had moderate to severe contamination from the host galaxy and bright stars in the field and are not used in this study. The successful grism observations are shown in Fig. 3. A log of the observations is given in Table 2.

### 2.3. *Swift* XRT Observations

The *Swift* XRT observations were obtained simultaneously with the UVOT and grism observations. X-ray counts were extracted from a circular region with an aperture of 10 pixel (24") radius centered at the position of the SN. The background was extracted locally from a source-free region of radius of 1' to account for detector and sky background, and for a low level of residual diffuse emission from the host galaxy.

<sup>17</sup> see [http://lheawww.gsfc.nasa.gov/users/immler/supernovae\\_list.html](http://lheawww.gsfc.nasa.gov/users/immler/supernovae_list.html) for a complete list of X-ray SNe and references

<sup>18</sup> <http://heasarc.gsfc.nasa.gov/docs/software/lheasoft/>

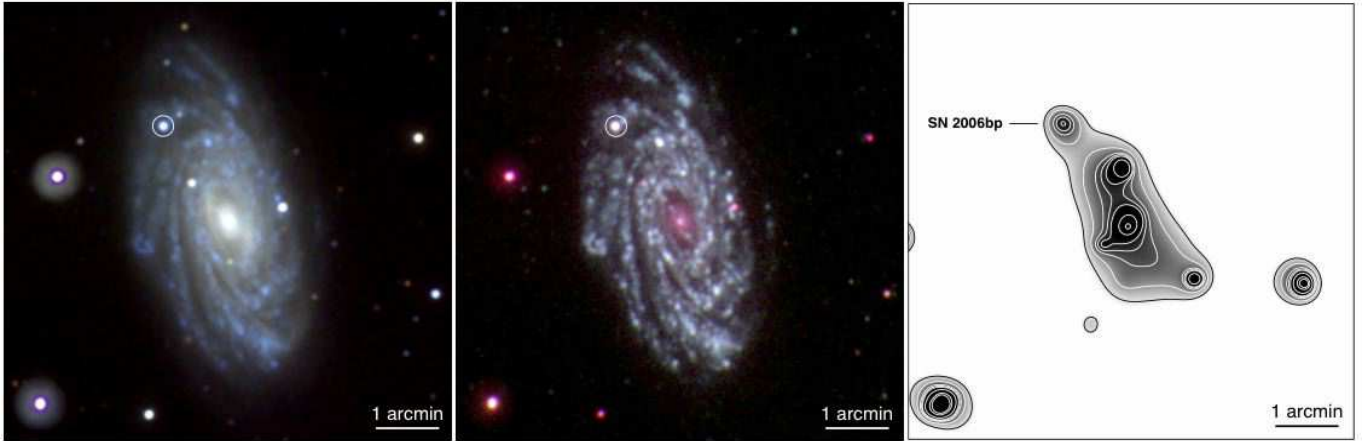


FIG. 1.— *Swift* optical, UV, and X-ray image of SN 2006bp and its host galaxy NGC 3953. **Left-hand panel:** *Swift* optical image, constructed from the UVOT *V* (750 s exposure time; red), *B* (1,966 s; green) and *U* (1,123 s; blue) filters obtained from 34 co-added images taken between 2006-04-10.54 UT and 2006-05-30.45 UT. The optical images are slightly smoothed with a Gaussian filter of 1.5 pixel (FWHM). The position of SN 2006bp is indicated by a white circle of 10 arcsec radius. The size of the image is 6.5 arcmin  $\times$  6.5 arcmin. **Middle panel:** The UV image was constructed from the co-added UVOT *UVW1* (750 s exposure time; red), *UVM2* (1,966 s; green) and *UVW2* (1,123 s; blue) filters obtained between 2006-04-10.54 UT and 2006-05-30.45 UT. The UV images are slightly smoothed with a Gaussian filter of 1.5 pixel (FWHM). Same scale as the left-hand panel. **Right-hand panel:** The (0.2–10 keV) X-ray image was constructed from the merged 41.4 ks XRT data and is adaptively smoothed with 0.6, 0.9, 1.5, 3, 6, 12, and 20 counts pixel $^{-1}$ . Same scale as the optical

TABLE 2  
UVOT GRISM OBSERVATIONS OF 2006BP

$t$ [d]	Sequence	Mode	$T_{\text{start}}$ [UT]	Exp [s]	$N_{\text{exp}}$
(1)	(2)	(3)	(4)	(5)	(6)
9	00030390020	UV	2006-04-18T07:30:28	2,431	2
12	00030390023	V	2006-04-21T06:10:22	2,688	2
14	00030390026	UV	2006-04-23T03:10:13	3252	4

NOTE. — (1) Days after the explosion of SN 2006bp (April 9, 2006); (2) *Swift* sequence number; (3) UVOT grism mode; (4) Exposure start time in unites of UT; (5) Exposure time in units of s; (6) Number of individual exposures.

#### 2.4. XMM-Newton Observation

An *XMM-Newton* European Photon Imaging Camera (EPIC) Director’s Discretionary Time (DDT) observation was performed on April 30.39 UT (PI Immler, OBSID 0311791401), corresponding to day 21 after the explosion. SAS<sup>19</sup> (version 7.0.0), FTOOLS<sup>20</sup> (version 6.1.1), and the latest *XMM-Newton* calibration products were used to analyze the *XMM-Newton* data. Inspection of the EPIC PN and MOS data for periods with a high particle background showed no contamination of the data, which resulted in clean exposure times of 21.2 ks for the PN and 22.9 ks for each of the two MOS instruments.

#### 2.5. VLA Radio Observation

Radio observations were performed with the VLA<sup>21</sup> at three epochs (days 2, 9, and 11) with a search for radio emission conducted within a radius of 10'' of the optical position (Nakano & Itagaki, 2006) using AIPS<sup>22</sup>.

<sup>19</sup> <http://xmm.vilspa.esa.es/sas/>

<sup>20</sup> <http://heasarc.gsfc.nasa.gov/docs/software.html>

<sup>21</sup> The VLA telescope of the National Radio Astronomy Observatory is operated by Associated Universities, Inc. under a cooperative agreement with the National Science Foundation

<sup>22</sup> <http://www.aoc.nrao.edu/aips/>

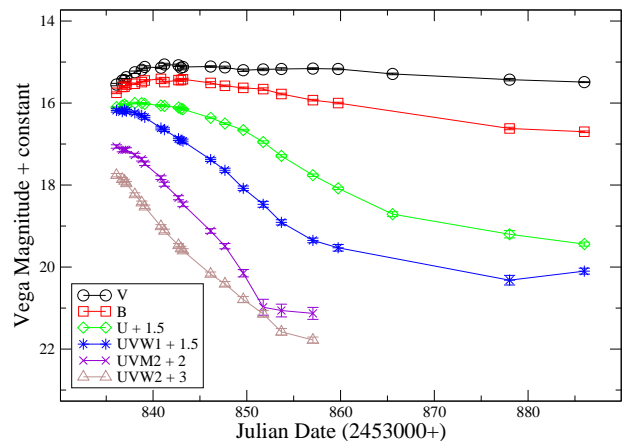


FIG. 2.— *Swift* UVOT lightcurve of SN 2006bp obtained in all six filters. The *U*, *UVW1*, *UVM2*, and *UVW2* lightcurves were shifted down vertically by 1.5, 1.5, 2, and 3 mag, respectively, to avoid overlap.

Upper limits ( $3\sigma$ ) to any radio flux density were established at  $< 0.414$  mJy on 2006 April 11.97 UT (spectral luminosity  $< 1.1 \times 10^{26}$  ergs $^{-1}$  Hz $^{-1}$  for an assumed distance of 14.9 Mpc) at 22.46 GHz (wavelength 1.3 cm) and  $< 0.281$  mJy at 8.460 GHz (wavelength 3.5 cm); on 2006 April 18.27 at  $< 0.498$  mJy at 14.94 GHz (wavelength 2.0 cm); and on 2006 April 20.16 at  $< 0.276$  mJy at 22.46 GHz and  $< 0.143$  mJy at 8.460 GHz (Kelley et al. 2006). Although only uncertain mass-loss rate estimates can be obtained from radio non-detections, under standard assumptions ( $v_w = 10$  km s $^{-1}$ ;  $v_s = 10^4$  km s $^{-1}$ ;  $T_{\text{CSM}} = 3\text{--}10 \times 10^4$  K;  $m = 1.0$ ; see, e.g. Weiler et al. 2002 and Lundqvist & Fransson 1988), the upper limit to the radio-determined pre-SN mass-loss rate is estimated to be  $10^{-6}$  to  $10^{-5}$   $M_{\odot}$  yr $^{-1}$ .

### 3. RESULTS

### 3.1. *Swift* UVOT Optical/UV Observations

The *Swift* V-band UVOT observations show that the SN reached its maximum brightness around day seven after the estimated time of explosion, faded slightly over the next few days and subsequently reached a plateau phase characteristic for type IIP SNe (see Fig. 2).

At increasingly shorter wavelengths, the SN shows an earlier maximum and steeper rates of decline. In the roughly linear period 5–15 days after the explosion, the decay slopes are approximately 0.21, 0.25, 0.16, 0.06, 0.02, and 0.01 mags/day in the *UVW2*, *UVM2*, *UVW1*, *U*, *B*, and *V* bands, respectively.

### 3.2. *Swift* and *XMM-Newton* X-ray Observations

An X-ray source is detected in the merged 41.4 ks *Swift* XRT observations obtained between days 1–12 after the explosion at R.A. = 11h53m56s.1, Decl. = +52°21′11″.1 (positional error 3″.5), consistent with the optical position of the SN. The aperture-, background- and vignetting-corrected net count rate is  $(1.3 \pm 0.3) \times 10^{-3}$  cts s<sup>-1</sup> (0.2–10 keV band). Two additional X-ray sources are detected within the  $D_{25}$  diameter of the host galaxy, as well as an X-ray source associated with the nucleus of the host galaxy (see Fig. 1). The chance probability of any of the three X-ray sources being within a radius of 3″.5 at the position of SN 2006bp is estimated to be  $1.5 \times 10^{-3}$ .

Adopting a thermal plasma spectrum with a temperature of  $kT = 10$  keV (see Fransson, Lundqvist & Chevalier 1996 and therein) and assuming a Galactic foreground column density with no intrinsic absorption ( $N_{\text{H}} = 1.58 \times 10^{20}$  cm<sup>-2</sup>; Dickey & Lockman 1990) gives a 0.2–10 keV X-ray band unabsorbed flux and luminosity of  $f_{0.2-10} = (6.8 \pm 1.6) \times 10^{-14}$  ergs cm<sup>-2</sup> s<sup>-1</sup> and  $L_{0.2-10} = (1.8 \pm 0.4) \times 10^{39}$  ergs s<sup>-1</sup>, respectively, for a distance of 14.9 Mpc ( $z = 0.00351$ , Verheijen & Sancisi 2001;  $H_0 = 71$  km s<sup>-1</sup> Mpc<sup>-1</sup>,  $\Omega_{\Lambda} = 2/3$ ,  $\Omega_{\text{m}} = 1/3$ ).

The SN is not detected in merged 23.1 ks XRT data obtained between days 12–31 after the explosion. The ( $3\sigma$ ) upper limit to the X-ray count rate is  $< 8.1 \times 10^{-4}$  cts s<sup>-1</sup> (0.2–10 keV), corresponding to an unabsorbed flux and luminosity of  $f_{0.2-10} < 4 \times 10^{-14}$  ergs cm<sup>-2</sup> s<sup>-1</sup> and  $L_{0.2-10} < 1 \times 10^{39}$  ergs s<sup>-1</sup>.

In order to probe the evolution of the X-ray emission in more detail, we subdivided the data taken before day 12 into two observations with similar exposure times of  $\approx 20$  ks each (see Table 3). Within the errors of the photon statistics, no significant decline is observed over the first 12 days after the explosion (see Fig. 4).

To follow the X-ray rate of decline over a longer period, an *XMM-Newton* observation was obtained on day 21 after the explosion. The SN is detected at a  $4.9\sigma$  level of confidence, with an EPIC PN net count rate of  $(3.0 \pm 0.6) \times 10^{-3}$  cts s<sup>-1</sup> (0.2–10 keV band), corresponding to an unabsorbed flux and luminosity of  $f_{0.2-10} = (1.4 \pm 0.3) \times 10^{-14}$  ergs cm<sup>-2</sup> s<sup>-1</sup> and  $L_{0.2-10} = (3.8 \pm 0.8) \times 10^{38}$  ergs s<sup>-1</sup>. A best fit X-ray rate of decline of  $L_{\text{x}} \propto t^{-n}$  with index  $n = 1.2 \pm 0.6$  is obtained using the *Swift* XRT and *XMM-Newton* detections. The X-ray lightcurve of SN 2006bp is given in Fig. 4. Due to the limited photon statistics of the *Swift* XRT and

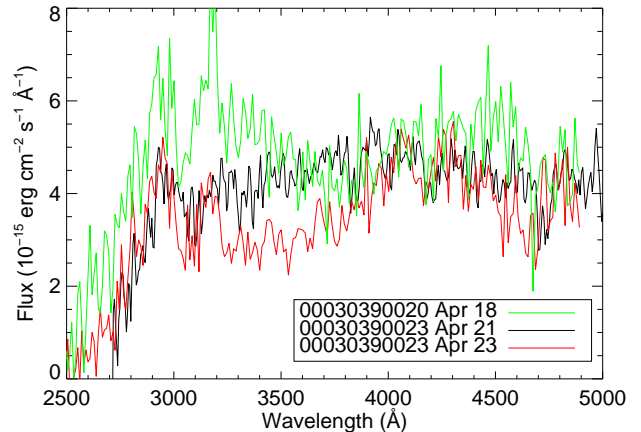


FIG. 3.— *Swift* UV grism observations of SN 2006bp obtained on April 18, 21, and 23, 2006, corresponding to days 9, 12, and 14 after the explosion.

*XMM-Newton* EPIC data, no detailed spectral fitting is possible.

## 4. DISCUSSION

### 4.1. Ultraviolet Emission

UV emission from SNe explosions can arise from different physical processes. The first photon signature from a core-collapse SN event is thought to be associated with shock break-out, which should manifest itself in a burst of light peaking in the X-rays and the far-UV (Ensmann & Burrows 1992; Blinnikov & Bartunov 1993; Blinnikov et al. 1998, 2000; Li 2006). The exact duration of this emission can be from hours to days, depending on the progenitor structure. Fast expansion of the ejecta and efficient radiative cooling at its ‘photosphere’ make this epoch short lived and therefore difficult to observe. At such early times, the object is not bright in the optical, and is thus usually still undetected. A SN is usually discovered when it becomes bright in the optical, but at this time the photosphere has cooled too much for X-ray emission. Observational evidence for a shock break-out was provided by *Swift* observations of the Gamma-Ray Burst (GRB) related to SN 2006aj (Campana et al. 2006), although this was probably mediated by a cocoon of material lost by the star before it collapsed.

UV emission has also been observed at early times ( $\lesssim 2$  weeks) in the photospheric phase of SN ejecta, emanating from the progenitor envelope layers that transition from thick to thin over time when the ejecta are still very hot (e.g. Mazzali 2000). The UV emission is typically strongest during early times (as in the spectrum of SN 1987A on day one; Pun et al. 1995) and fades substantially over the course of a few days (weak UV emission has been detected in an HST observation of SN 1993J, 18 days after the explosion; Jeffery et al. 1994; Baron et al. 1994). At later times ( $\gtrsim$  weeks), UV emission is in general associated with the interaction of the ejecta with the CSM (Fransson et al. 1987, 2002; Pun et al. 2002).

The UV is therefore a very sensitive spectral probe of the fast changing conditions in the SN expanding photosphere during the earliest phases.

The first observation of SN 2006bp shows a spectral energy distribution (SED) peak in the UV, rather than the optical (Fig. 5), which supports that the SN was de-

TABLE 3  
X-RAY OBSERVATIONS OF 2006BP

Day after Explosion	Instrument	Exposure [ks]	S/N [ $\sigma$ ]	Rate [ $10^{-3}$ ]	$f_x$ [ $10^{-14}$ ]	$L_x$ [ $10^{39}$ ]
(1)	(2)	(3)	(4)	(5)	(6)	(7)
1–5	<i>Swift</i> XRT	20.0	4.4	$1.31 \pm 0.30$	$6.94 \pm 1.58$	$1.84 \pm 0.42$
6–12	<i>Swift</i> XRT	21.5	4.4	$1.25 \pm 0.29$	$6.58 \pm 1.52$	$1.75 \pm 0.40$
13–31	<i>Swift</i> XRT	23.1	< 3	< 0.81	< 4.00	< 1.06
21	XMM EPIC PN	21.2	4.9	$3.0 \pm 0.6$	$1.4 \pm 0.3$	$0.38 \pm 0.08$

NOTE. — (1) Days after the explosion of SN 2006bp (April 9, 2006); (2) Instrument used; (3) Exposure time in units of ks; (4) Significance of source detection in units of Gaussian sigma; (5) 0.2–10 keV count rate in units of cts ks $^{-1}$ ; (6) 0.2–10 keV X-ray band unabsorbed flux in units of  $10^{-14}$  ergs cm $^{-2}$  s $^{-1}$ ; (7) 0.2–10 keV X-ray band luminosity in units of  $10^{39}$  ergs s $^{-1}$ .

tection very early. Thirty-five observations finely sample the lightcurve over 51 days after discovery, revealing a flux variation in the UV by two orders of magnitude. The redward shift of the SED stems from cooling of the photosphere. There is a direct effect in the reduction of the equivalent blackbody (or effective/electron) temperature (e.g. Mazzali & Chugai 1995), but the main effect is caused by the shift of the opacity from species of higher to lower ionization, as discussed in Eastman & Kirshner (1989) and Dessart & Hillier (2005, 2006).

The main physical process affecting the UV flux distribution is line blanketing (e.g. Lentz et al. 2000, Mazzali 2000). Metal lines, especially lines of FeII and FeIII, are very numerous in the UV, and the velocity dispersion in the ejecta causes these lines to act as a blanket that blocks the UV flux. Photons absorbed in the UV are re-emitted at visible wavelengths, where they can more easily escape (e.g. Mazzali & Lucy 1993, Mazzali 2000). Thus the UV flux is determined by the ionization state of the SN envelope as well as by its metal content. Since on average UV FeIII lines are redder than FeII lines, the sudden transition from FeIII to FeII when hydrogen recombines in the ejecta of a type II SN shifts the region where line-blanketing is most effective and affects the UV spectrum dramatically (see Figs 1, 3, and 5 in Dessart & Hillier 2005). This onset of line blanketing is evident in the UV spectra of SN 2006bp as observed by *Swift* (see Fig. 3). The corresponding forest of overlapping lines gives an apparently continuous source of light blocking: at early times, FeIII blanketing operates most strongly between 1500 and 2000Å, while at later times, FeII blanketing affects the entire UV range. Combined with this dominant background opacity are a few strong resonance lines of less abundant metals, e.g. MgII 2800 Å, which are only visible while metal line-blanketing is moderate.

The SED evolution supports the current understanding of the photospheric phase of type II SNe, however, UV coverage will provide a more extended spectroscopic and photometric analysis. In particular, the unsaturated metal line blanketing together with the fast changing UV SED provides additional constraints on the temperature evolution, the ejecta ionization and composition, and, importantly, on reddening, that optical observations alone do not guarantee. This will be the subject of a forthcoming study (Dessart in preparation).

#### 4.2. X-Ray Emission

X-ray emission from young (days to weeks) SNe can be produced by the radioactive decay products of the ejecta, inverse Compton scattering of photospheric photons off relativistic electrons produced during the explosion, as well as by the interaction of the SN shock with the ambient CSM (forward shock) and SN ejecta (reverse shock).

While several of the emission lines characteristic of the radioactive decay products have been observed in SN 1987A (e.g., McCray 1993), the total X-ray output is five orders of magnitude lower ( $\approx 10^{34}$  ergs s $^{-1}$ ) than the observed X-ray luminosity of SN 2006bp. Therefore, no significant contribution of the radioactive decay products to the total X-ray luminosity of SN 2006bp is expected. Recent simulations of the expected X-ray emission from Compton-scattered  $\gamma$ -rays of the radioactive decay products of the SN ejecta for SN 2005ke at early epochs (days) also shows the expected X-ray luminosity to be in the range  $10^{33}$ – $10^{34}$  ergs s $^{-1}$  (Immler et al. 2006), well below the observed X-ray luminosity of SN 2006bp.

This leaves either inverse Compton scattering or CSM interaction as the likely source of the detected X-ray emission.

Since type IIP SNe have a prolonged plateau period with high optical output associated with hydrogen recombination in the progenitor envelope, inverse Compton cooling of the relativistic electrons produced during the explosion by the photospheric photons might be important. Up-scattering of the optical photons to energies in the X-ray range (depending on the Lorentz factor and effective temperature of the photospheric emission) could produce a detectable X-ray flux during the first few days after outburst.

Chevalier, Fransson & Nymark (2006) have shown that the X-ray luminosity of inverse Compton emission takes the form  $\frac{dL_{IC}}{dE} \approx 8.8 \times 10^{38} \epsilon_r \gamma_{\min} E_{\text{keV}}^{-1} \left(\frac{\dot{M}_{-6}}{v_w}\right) v_{s4} \left(\frac{L_{\text{bol}}(t)}{10^{42} \text{ ergs s}^{-1}}\right) \left(\frac{t}{10 \text{ days}}\right)^{-1} \frac{\text{ergs}}{\text{s keV}}$ , where  $\epsilon_r$  is the fraction of the postshock energy density that is in relativistic electrons,  $\gamma_{\min}$  the minimum Lorentz factor of the relativistic electrons,  $\dot{M}_{-6}$  the mass-loss rate (in units of  $10^{-6} M_{\odot} \text{ yr}^{-1}$ ),  $v_w$  the wind velocity (in units of km s $^{-1}$ ),  $v_{s4}$  the SN shock velocity (in units of 10,000 km s $^{-1}$ ), and  $L_{\text{bol}}(t)$  the bolometric luminosity at time  $t$  after the explosion. Assuming a mass-loss rate of  $\dot{M} = 2 \times 10^{-6} M_{\odot} \text{ yr}^{-1}$  ( $v_w/10 \text{ km s}^{-1}$ ) (see below), a shock velocity of 15,000 km s $^{-1}$ , and a bolometric luminosity of  $L_{\text{bol}} = 10^{42}$  ergs s $^{-1}$ , we

estimate a monochromatic X-ray luminosity from inverse Compton scattering at 1 keV (near the peak of the *Swift* XRT and *XMM-Newton* EPIC response) of  $L_x \approx \epsilon_r \gamma_{\min} 4 \times 10^{39} \text{ ergs s}^{-1}$ . The bolometric luminosity is justified by the modeling of SNe IIP lightcurves (e.g., Chieffi et al. 2003).

Since the value for  $\epsilon_r$  is expected to be in the range  $\approx 0.01\text{--}0.1$ , a Lorentz factor of  $\gamma_{\min} \approx 10\text{--}100$  is needed to satisfy the condition that all of the observed X-rays are due to inverse Compton scattering. As the most plausible value for the Lorentz factor for the shock velocities of SNe IIP is  $\approx 1$  (Chevalier, Fransson & Nymark 2006), inverse Compton scattering is unlikely to account for the observed X-ray emission of SN 2006bp, although it cannot be ruled out entirely.

Alternatively, the X-ray emission might be caused by the interaction of the shock with the CSM, deposited by the progenitor’s stellar wind. Of all 26 SNe detected in X-rays over the past three decades, the importance of inverse Compton scattering has only been discussed for the type Ic SNe 1998bw (Pian et al. 2000) and 2002ap (Bjornsson & Fransson 2004), while the remaining X-ray SNe have been discussed in the context of thermal emission [apart from the early emission of SN 1987A, see Park et al. (2006) and references therein].

Assuming a constant mass loss rate  $\dot{M}$  and wind velocity  $v_w$  from the progenitor’s companion, the thermal X-ray luminosity of the forward shock region is  $L_x = 1/(\pi m^2) \Lambda(T) \times (\dot{M}/v_w)^2 \times (v_s t)^{-1}$  (Immler et al. 2006), where  $m$  is the mean mass per particle ( $2.1 \times 10^{-24}$  g for a H+He plasma),  $\Lambda(T)$  the cooling function of the heated plasma at temperature  $T = 1.36 \times 10^9 (n-3)^2 / (n-2)^2 (v_s / [10^4 \text{ km/s}])^2$  K (Chevalier & Fransson 2003),  $n$  is the ejecta density parameter (in the range 7–12) and  $v_s$  the shock velocity. Adopting an effective cooling function of  $\Lambda_{\text{ff}} = 2.4 \times 10^{-27} g_{\text{ff}} T_e^{0.5} \text{ ergs cm}^3 \text{ s}^{-1}$  (Chevalier & Fransson 2003) for an optically thin thermal plasma with a temperature of  $T$  for the forward shock, where  $g_{\text{ff}}$  is the free-free Gaunt factor, and  $v_s = 15,000 \text{ km s}^{-1}$ , a mass-loss rate of  $\dot{M} \approx 1 \times 10^{-5} M_{\odot} \text{ yr}^{-1} (v_w / 10 \text{ km s}^{-1})$  with an uncertainty of a factor of 2–3 is obtained. Assuming different plasma temperatures in the range  $10^7\text{--}10^9$  K would lead to changes in the emission measure by a factor of three. The X-ray luminosity from shock-heated plasma behind the reverse shock is assumed to be small compared to that of the forward shock since the expanding shell is still optically thick at such an early epoch. Since only high-quality X-ray spectra could give a conclusive answer to the contribution of the reverse shock to the total X-ray luminosity, our inferred mass-loss rate represents an upper limit. In case absorption is small and the bulk of the thermal emission originates in the reverse shock, the value of  $\dot{M}$  is reduced by a factor of up to 10 assuming an ejecta density parameter of  $n = 10$  (with a range between 7 and 12; see equation 33 in Chevalier 1982).

While other core-collapse SN (type Ib/c and II) progenitors can produce mass-loss rates as high as  $10^{-5}$  to  $10^{-3} M_{\odot} \text{ yr}^{-1}$  due to the high masses and strong stellar winds of the progenitor stars, the mass-loss rate of the SN 2006bp progenitor is similar to those of other type IIP SNe: a recent study of the thermal X-ray and radio syn-

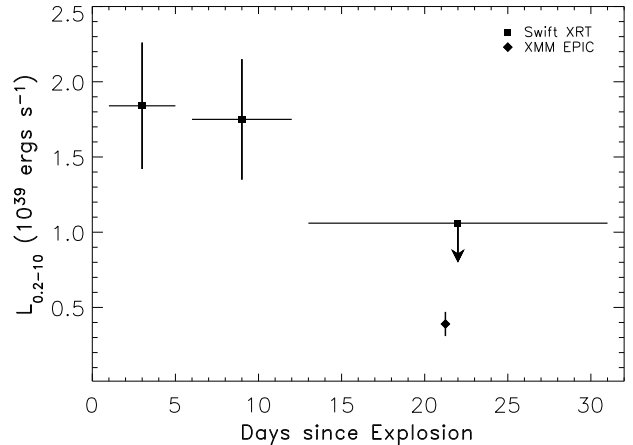


FIG. 4.— X-ray lightcurve (0.2–10 keV) of SN 2006bp as observed with the *Swift* XRT and *XMM-Newton* EPIC instruments. The time is given in days after the outburst (April 9, 2006). Vertical error bars are statistical  $1\sigma$  errors; horizontal error bars indicate the periods covered by the observations (which are not contiguous). The *Swift* XRT upper limit from day 13–31 is at a  $3\sigma$  level of confidence.

chrotron emission of a sample of type IIP SNe (1999em, 1999gi, 2002hh, 2003gd, 2004dj, 2004et) gave mass-loss rate estimates of a few  $10^{-6} M_{\odot} \text{ yr}^{-1}$  (Chevalier, Fransson & Nymark 2006), characteristic of red supergiant progenitors, assuming stellar wind velocities for red supergiants of  $10\text{--}15 \text{ km s}^{-1}$ . Comparison shows that the SN 2006bp progenitor had a mass-loss rate similar to the lowest in this sample (SNe 1999gi, 2004dj) and an mass around  $\approx 12\text{--}15 M_{\odot}$  prior to the explosion (see Fig. 1 in Chevalier, Fransson & Nymark 2006) in case the X-ray emission was dominated by the reverse shock.

CSM interaction gives an expected  $t^{-1}$  decline of the X-ray flux, consistent with the observed rate of decline ( $t^{-n}$  with index  $n = 1.2 \pm 0.6$ ). Inverse Compton scattering, on the other hand, only gives a  $t^{-1}$  decline in case of  $L_{\text{bol}}(t)$  is constant over time (as in the UVOT  $V$ -band light curve). However, at early times the blue/UV emission, which shows a fast rate of decline, contributes significantly to the bolometric luminosity, which leads to a faster X-ray rate of decline for Inverse Compton Scattering. Due to the large errors associated with the X-ray rate of decline, inverse Compton scattering cannot be entirely ruled out, but is a less likely scenario for the production of the observed X-rays.

The distinguishing characteristic of the two emission processes is their spectrum (power law vs thermal plasma). In the absence of high-quality spectra for the *Swift* XRT and *XMM-Newton* EPIC data, such a distinction cannot be made since the *XMM-Newton* EPIC data are equally well fit (using Cash statistics; Cash 1979) by a power law (best fit photon index  $\Gamma = 1.6_{-0.7}^{+1.2}$ ;  $\chi^2 = 42.6$ , d.o.f. = 52), a thermal plasma spectrum (best fit temperature  $kT = 1.7\text{--}27$  keV, consistent with our spectral assumptions to infer fluxes;  $\chi^2 = 42.3$ , d.o.f. = 52) and a thermal bremsstrahlung spectrum (best fit temperature  $kT = 1.0\text{--}179$  keV;  $\chi^2 = 41.4$ , d.o.f. = 52).

## 5. SUMMARY

Starting at an age of  $\approx 1$  day after the outburst, our *Swift* observations of SN 2006bp represent the earliest

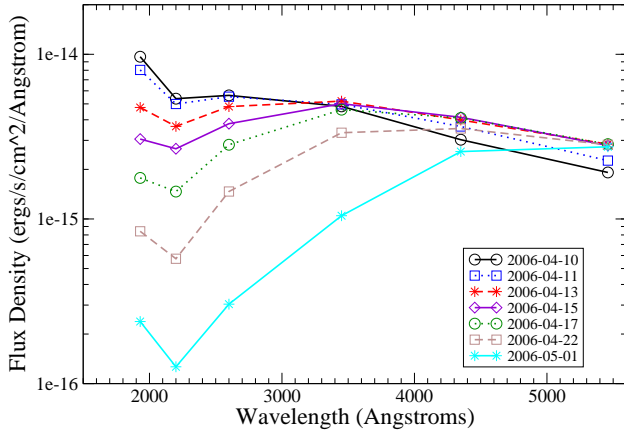


FIG. 5.— Evolution of the spectral energy distribution (SED) of SN 2006bp in the optical/UV wavelength band. The SED was produced from near-simultaneous UVOT observations in all six filters obtained between days 1 and 26 after the explosion (from top to bottom).

X-ray observation and detection of a SN to date, apart from two explosions which were accompanied by a  $\gamma$ -ray signal (as in the case of SN 1998bw/GRB 980425, which *BeppoSAX* started observing 12 hrs after the outburst [Pian et al. 2000] and SN 2006aj/GRB 060218, for which prompt X-ray emission was detected [Campana et al. 2006]). SN 2006bp faded below the *Swift* XRT sensitivity limit within less than two weeks and a more sensitive *XMM-Newton* observation recovered the SN three weeks after its explosion. Broad-band SEDs and in particular UV spectra of SNe show the importance and give insights into line blanketing during the early phase in the evolution.

Currently, *Swift* is the only telescope capable of revealing the fast changes in the UV flux from SN explosions, offering sensitive constraints on the ionization state in the continuum and line formation region of the ejecta, the sources of metal line-blanketing. By extending the spectral coverage, this provides stronger constraints on the reddening, and complementary information, to what can be deduced from optical observations alone. While there is ample evidence for diversity in type II SN optical spectra, *Swift* observations can be used to address the existence of a corresponding diversity in the UV range.

The detection of SN 2006bp in X-rays at such an early epoch, as well as the detection of its fast optical/UV spectral evolution was made possible by the quick response of the *Swift* satellite, and underlines the need for rapid observations of SNe in the UV and in X-rays. It should be pointed out that the response time of all previous X-ray observations of SNe (with missions such as *Einstein*, *ASCA*, *ROSAT*, *Chandra*, and *XMM-Newton*) were in the range between  $> 4$  days (SN 2002ap) and a few weeks. The bulk of all X-ray observations took place weeks to months after the explosions. Therefore, if SN 2006bp is more typical for a larger sample of core-collapse SNe, then the early production of X-rays would have been missed in each of the previous cases. The response time of our ongoing *Swift* observing program to study the prompt emission of SNe across the optical, UV, and X-rays is currently only limited by the time lag between the explosion of a SN and its discovery at optical wavelengths and timely alert by the community.

We gratefully acknowledge support provided by STScI grant HST-GO-10182.75-A (P.A.M.), NASA Chandra Postdoctoral Fellowship grant PF4-50035 (D.P.), and NSF grant AST-0307366 (R.A.C.). L.D acknowledges support for this work from the Scientific Discovery through Advanced Computing (SciDAC) program of the DOE, grant DE-FC02-01ER41184 and from the NSF under grant AST-0504947. K.W.W. thanks the Office of Naval Research for the 6.1 funding supporting this research. C.J.S. is a Cottrell Scholar of Research Corporation and work on this project has been supported by the NASA Wisconsin Space Grant Consortium. This work is sponsored at The Pennsylvania State University by NASA contract NAS5-00136. We wish to thank N. Schartel and the *XMM-Newton* SOC for approving and scheduling a *XMM-Newton* DDT observation. The research has made use of the NASA/IPAC Extragalactic Database (NED) which is operated by the Jet Propulsion Laboratory, California Institute of Technology, under contract with the National Aeronautics and Space Administration.

## REFERENCES

- Baron, E., Hauschildt, P. H., & Branch, D. 1994, *ApJ* 426, 334  
 Bjornsson, C.-I., & Fransson, C. 2004, *ApJ* 606, 823  
 Blinnikov, S., & Bartunov, O. S. 1993, *A&A* 273, 106  
 Blinnikov, S., Eastman, R. G., Bartunov, O. S., Popolitov, V. A., & Woosley, S. E. 1998, *ApJ* 496, 454  
 Blinnikov, S., Lundqvist, P., Bartunov, O. S., Nomoto, K., & Iwamoto, K. 2000, *ApJ* 532, 1132  
 Burrows, D. N. et al. 2005, *Space Science Reviews* 120, 165  
 Campana, S. et al. 2006, *Nature* 442, 1008  
 Cash, W. 1979, *ApJ* 228, 939  
 Chevalier, R. A. 1982, *ApJ* 259, 302  
 Chevalier, R. A. & Fransson, C. 2003, in *Supernovae and Gamma-Ray Bursters* (ed K. Weiler), *Lecture Notes in Physics*, 598, 171  
 Chevalier, R. A., Fransson, C., Nymark, T. K. 2006, *ApJ* 641, 1029  
 Chieffi, A., Domínguez, I., Höflich, P., Limongi, M., Straniero, O. 2003, *MNRAS* 345, 111  
 Dessart, L., & Hillier, D. J. 2006, *A&A* 447, 691  
 Dessart, L., & Hillier, D. J. 2005, *A&A* 437, 667  
 Dickey, J. M., Lockman, F. J. 1990, *ARA&A* 28, 215  
 Eastman, R. G., & Kirshner, R. P. 1989, *ApJ* 347, 771  
 Ensmann, L., & Burrows, A. 1992, *ApJ* 393, 742  
 Fransson, C., Grewing, M., Cassatella, A., Wamsteker, W., & Panagia, N. 1987, *A&A* 177, L33  
 Fransson, C., Lundqvist, P., Chevalier, R. A. 1996, *ApJ* 461, 993  
 Fransson, C., et al. 2002, *ApJ* 572, 350  
 Gehrels, N. et al. 2004, *ApJ* 611, 1005  
 Heger, A., Fryer, C. L., Woosley, S. E., Langer, N., Hartman, D. H. 2003, *ApJ* 591, 288  
 Immler, S., Wilson, A. S., Terashima, Y. 2002, *ApJ* 573, L27  
 Immler, S., Lewin, W. 2003, in *Supernovae and Gamma-Ray Bursters* (ed K. Weiler), *Lecture Notes in Physics*, 598, 91  
 Immler, S., Brown, P., Milne, P. 2006, *ATel* 793, 1  
 Immler, S. et al. 2006, *ApJ* 648, L119  
 Jeffery, D. J., et al. 1994, *ApJ* 421, L27

- Kelley, M. T., Stockdale, C. J., Sramek, R. A., Weiler, K. W.,  
Immler, S., Panagia, N., van Dyk, S. D. 2006, CBET 495, 1
- Lentz, E. J., Baron, E., Branch, D., Hauschildt, P. H., & Nugent,  
P. E. 2000, ApJ 530, 966
- Li, Li-Xin, 2006, accepted for publication by MNRAS  
(astro-ph/0605387)
- Lundqvist, P., & Fransson, C. 1988, A&A 192, 221
- Mazzali, P. A. 2000, A&A 363, 705
- Mazzali, P. A., & Chugai, N. N. 1995, A&A 303, 118
- Mazzali, P. A., & Lucy, L. B. 1993, A&A 279, 447
- McCray, R. 1993, ARA&A 31, 175
- Nakamo, S., Itagaki, K. 2006, CBET 470 1
- Park, S., et al. 2006, ApJ 646, 1001
- Pian, E., et al. 2000, ApJ 536, 778
- Pun, C. S. J., et al. 2002, ApJ 572, 906
- Pun, C. S. J., et al. 1995, ApJ 99, 223
- Quimby, R., Brown, P., Caldwell, J., Rostopchin, S. 2006, CBET  
471, 1
- Roming, P. W. A., et al. 2005, Space Science Reviews 120, 95
- Verheijen, M. A. W., Sancisi, R. 2001, ApJ 370, 765
- Weiler, K. W., Panagia, N., Montes, M. J., Sramek, R. A. 2002,  
ARA&A 40, 387